Biointerface Research in Applied Chemistry
Open-Access Journal (ISSN: 2069-5837)

Article
Volume 13, Issue 4, 2023, 357
https://doi.org/10.33263/BRIAC134.357

Computational Insights in the Spectrophotometrically Analyzed Niobium (V)- 3-Hydroxy-2-(4-methylphenyl)-4H-chromen-4-one Complex using DFT Method

Chetna Dhonchak [1], Nivedita Agnihotri [1,*], Akshay Kumar [2], Abhinay Thakur [3], Ashish Kumar [3]

[1] Department of Chemistry, Maharishi Markandeshwar (Deemed to be University), Mullana, Ambala-133207, Haryana, India
[2] Department of Chemistry, Dyal Singh College, Karnal-132001, Haryana, India
[3] Department of Chemistry, Faculty of Technology and Science, Lovely Professional University, Phagwara-144411, Punjab, India
* Correspondence: nivagni11@gmail (N.A.);

Scopus Author ID 7004253795
Received: 16.05.2022; Accepted: 21.06.2022; Published: 17.09.2022

Abstract: Using 3-hydroxy-2-(4-methylphenyl)-4H-chromen-4-one (HMC) as a complexing agent in an acidic medium, a simple, quick, highly sensitive, and selective approach for the extractive spectrophotometric measurement of micro quantities of niobium (V) is developed. The yellowish 1:3 complex can be extracted 100 % in dichloromethane (DCM), attaining maximum absorbance in the wavelength range 388-407 nm. At 400 nm, the selected wavelength, the approach follows a linear calibration curve up to 2.2 g Nb (V) ml-1 and 0.395-1.78 ppm Nb (V) as identified from the Ringbom Plot with molar absorptivity, specific absorptivity, and Sandell's sensitivity of 4.926 × 104 l mol-1 cm-1, 0.5302 ml g-1 cm-1 and 0.0019 µg Nb cm-2, respectively. With a correlation coefficient of 0.9994, the linear regression equation is Y = 0.514 X + 0.016. The method's detection limit is 0.0698 µg ml-1. The presented determination of pentavalent niobium is unaffected by 33 cations and 22 anions/complexing agents. The approach has good reproducibility and can be used to determine niobium in a satisfactory manner. The analytical study has been correlated well with the theoretical approach of Density Functional Theory (DFT) for quantum chemical calculations. DFT effectively helped determine and interpret the chemical behavior of the obtained Nb(V)-HMC complex, explaining its stability and reactivity pattern.

Keywords: niobium (V); 3-Hydroxy-2-(4-methylphenyl)-4H-chromen-4-one; extraction; spectrophotometric determination; DFT.

1. Introduction

The use of niobium as an alloying element to high strength low alloy steel and stainless steel for oil and gas pipelines, car and truck bodies, architectural needs, tool steels, ship hulls, and railroad tracks accounts for the majority of its usage. Although niobium has several uses, the maximum of it is used to make high-grade structural steel [1-3]. Niobium and some of its alloys are physiologically inert and hypoallergenic. For this reason, niobium is used in prosthetics and implant devices, such as pacemakers [4]. Niobium treated with sodium hydroxide forms a porous layer that aids osseointegration [5]. Thus, a reliable and specific evaluation of the metal is an important venture.

Spectrophotometric approaches are favored for micro determination of the elements in a wide range of samples, owing to their ease of use and excellent reliability [6-12]. Although numerous methods for niobium determination have been developed in the past based on diverse reactions with various organic/inorganic ligands yet, they have been afflicted by multiple interferences as well as other essential factors such as the basic requirements of the procedures, sensitivity, and selectivity that limit their usefulness [13-17]. Thus, for the reasons outlined in particular, it is a continuous process to seek better strategies to reduce interference while simultaneously improving sensitivity, regardless of whether this is a new or modified method.

In the following study, a new chromone called 3-hydroxy-2-(4-methylphenyl)-4H-chromen-4-one (HMC) was complexed with Niobium (V) to produce a yellow-colored complex that was examined spectrophotometrically. Structural elucidation of HMC and its Nb (V) complex was performed satisfactorily using Density functional simulations (DFT) that nowadays is a well in used technique to study electronic properties of the coordination complexes in chemistry [18-22]. The use of DFT features frontier molecular orbital energies, reactivity parameters, and ESP diagrams which have aided in a better understanding of the ligand and complex structures.

2. Materials and Methods

2.1. Instrumentation, reagents, and solutions.

For absorbance estimations and spectral analyses, a dual beam UV-Visible spectrophotometer (2375; Electronics India) with 10 mm coordinated quartz cells is employed.

By fusing a carefully weighed amount (0.1430 g) of niobium pentaoxide, Nb_2O_5, with 3g potassium bisulfate in a crucible made of silica, followed by dissolving the melt in a hot 5% tartaric acid solution, cooling and adjusting to the desired consistency with 100 ml distilled water, a standard 1 mg ml-1stock solution of Nb (V) was prepared. Working solutions of µg ml-1 concentrations were prepared by diluting the stock solution with 2 % tartaric acid.

The required solutions of distinct metal ions are made by dissolving their soluble chemically pure sodium or potassium salts in doubly distilled water or diluting mineral acids to achieve a metal ion concentration up to 10 mg ml^{-1}.

By the earlier reported detailed method [23-25], HMC [molecular formula = C16H12O3, molar mass = 252 g mol-1, melting point = 206 °C, Figure 1] was synthesized and its 0.2 g per 100 ml (0.2% w/v) fresh ethanolic solution is used for determination of Nb (V).

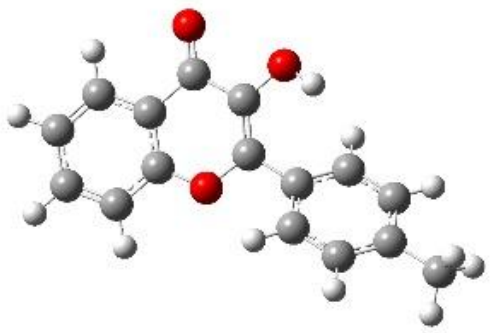

Figure 1. Structure of HMC.

A freshly prepared aqueous HClO4 (8 M) solution is employed to achieve the acidic conditions set for complex formation. DCM (AR, CDH) is used as such for the extraction of the complex.

2.2. Samples.

The method's validity is ensured by the successful analysis of the following samples.

a. Synthetic samples: Synthetic samples are prepared by mixing milligram amounts of niobium (V) with other metal ions in reasonable proportions (Table 1).

b. Natural and industrial samples: The samples of reverberatory flue dust and water (from different sources) are brought into desired solutions of the set concentrations following the procedures reported earlier [16]. However, the BCS 261/1 steel sample is prepared by subjecting 0.05 g of the sample in aqua regia (conc. HCl: conc. HNO_3; 3:1) to slow heating on a sand bath.10 ml of deionized water was added after evaporating the contents to dryness, along with its acidification and dissolution in 50 ml of 2.8 M $HClO_4$. Niobium is then analyzed by the proposed method by taking out desired aliquots from all the thus prepared solutions, respectively (Table 1).

Table 1. Analysis of various synthetic and technical samples.

S No.	Sample Composition		Nb (V) found (µg /10ml)**
	Matrix*	Nb (V) added (µg/10ml)	
1	Mn(2),Co(5), Zn(5)	8	8.13±0.020
2	Pt(0.5), Pd(0.5), Al(1)	12	12.05±0.032
3	Mo(0.05), W(0.2), Fe^{III}(0.5)[a]	10	10.14±0.029
4	Zr(0.5), Pd(0.5), As(0.5)	8	7.99±0.024
5	Cu(2), Pb(5), Hg(2)	10	9.95±0.033
6	Mg(5), Ce(1), Ru(0.5)	8	8.15±0.009
7	Cr^{VI}(0.5), Bi(0.5), Ti(0.5)	12	12.22±0.017
8	Ir(0.5),Fe^{II}(0.5),Au(0.5)	15	15.10±0.008
9	V(0.05),La(0.5),Sr(0.5)[b]	15	14.93±0.055
10	Se(2), Mg(5), Ru(0.5)	20	20.09±0.011
11	Cd(5), Ba(5), Fe^{III}(0.5)	12	11.88±0.023
12	Ag(5), Sr(0.5), Cr^{III}(0.1)	8	8.07±0.038
13	Water: I) Tap Water II) Ground Water	10 15	9.96±0.024 15.11±0.017
14	Reverberatory Flue Dust	8	7.95±0.031
15	BCS (261/1)[a]	0.91%[c]	0.92±0.016

Figure in parentheses indicates the amount of metal ion in mg 10 ml-1. **Average of triplicate analyses ± SD.
[a]In presence of 100 mg Potassium thiocyanate; [b]In presence of 100 mg Ascorbic acid; [c]Certified Value.

2.3. Quantum chemical insights for Nb(V)-HMC complex.

DFT is a computational quantum chemical modeling method used in physics, chemistry, and materials science to study the electronic properties or nuclear structure (principally the ground state) of many-body systems, including atoms, molecules, and condensed phases. The theory is widely regarded as a prominent post-Hartree–Fock (HF) technique for computing molecular structures and energies ab initio and has been proven to be very effective in understanding molecular electronic structures [6,26,27]. The Gaussian09 package [28] was used to perform DFT and theoretical calculations on the ligand HMC and the Nb(V)-HMC complex. The basis set for HMC is B3LYP, 6-311G, ++, d, p, Charge 0 with singlet spin, whereas the optimization basis set for Nb(V)-HMC complex is B3LYP, LanL2DZ, Charge 0 with singlet spin [29]. For a better structural comprehension of HMC and its Nb(V) complex, quantum chemical characteristics such as energies of highest occupied molecular orbital (HOMO), lowest unoccupied molecular orbital (LUMO), and HOMO-LUMO energy

gap (ΔE_{gap}) were computed. In addition, dipole moment (μ) prediction is critical in discussing molecule stability in polar environments. The dipole moment values and the energy gaps between the highest occupied molecular orbital and the lowest empty molecular orbital reflect diverse charge-transfer possibilities inside the molecules under consideration. Increased dipole moments reflect the increased stability with an electron-donating group in polar solvents [30]. Finally, global reactivity descriptors and Electrostatic surface potential (ESP) diagrams were used to validate the experimental findings and better understand the ligand and its interaction with pentavalent niobium metal.

2.4. Procedure for extraction and determination.

An aliquot of the working solution containing up to 22 µg of Nb (V) is placed in a 125 ml separating funnel. The addition is made of sufficient $HClO_4$ solution to maintain the acidity of the aqueous phase in the range 2.24-3.28 M followed by 2 ml of 0.2% (w/v) solution of HMC in ethanol in a total aqueous volume of 10 ml. The aqueous content thus prepared is equilibrated once with 10 ml of DCM for 30 seconds. After phase separation, the organic layer is filtered into a 10 ml volumetric flask through a Whatman filter paper No.41 (9 cm diameter) and diluted up to the mark with pure DCM. The contents are gently mixed, and the absorbance of the yellow extract is measured at 400 nm against a blank solution prepared analogously using a pair of 1 cm quartz cuvettes. The amount of niobium is determined from the calibration curve obtained by the above-said procedure.

Modifications for V(V) and Mo(VI): Up to 0.1 mg of V(V) and Mo(VI) are masked with 100 mg of ascorbic acid and 100 mg of potassium thiocyanate, respectively, when added prior to the addition of reagent in 10 ml water phase.

3. Results and Discussion

In a perchloric acid medium, HMC reacts with niobium in the pentavalent state to give a yellow-colored, extractable into DCM, stable complex (stability more than 4 days), giving a consistent absorbance in the range 388-407 nm. When combined with other media (acidic and basic) than HClO4, complexation produced faded tones and hence a lower optical density value, as shown in Table 2.

Table 2. Effect of nature of medium on the absorbance of Nb(V) - HMC complex.

Acid*	$HClO_4$	HCl	H_2SO_4	CH_3COOH	H_3PO_4	$NaHCO_3$	Na_2CO_3	NH_3
Absorbance	0.268	0.209	0.198	0.125	0.097	0.045	0.028	0.020

*Nb(V) = 10µg; Acidity/Basicity of the aqueous phase = 0.4 M; HMC [0.2% (w/v) in ethanol] = 1.5ml; aqueous volume = solvent volume = 10ml; solvent = chloroform; equilibration time = 45 seconds; λmax= 400 nm.

Disparate solvents were explored to examine the extraction conduct of the formed Nb(V)-HMC complex exhibiting variation in extraction tendency, as indicated in Table 3.

Table 3. Effect of solvents on the absorbance of Nb (V) - HMC complex.

Solvent*	**Absorbance**
DCM	0.282
Carbon tetrachloride	0.275
Chloroform	0.268
Toluene	0.173
1,2-Dichloroethane	0.128
Isobutyl methyl ketone	0.121
Benzene	0.068
Amyl acetate	0.037

Solvent*	Absorbance
Ethyl acetate	0.028
Cyclohexane	0.012

*Nb(V) = 10 µg; Acidity of the aqueous phase = 0.4 M; HMC [0.2% (w/v) in ethanol] = 1.5 ml; aqueous volume = solvent volume = 10 ml; solvent = variable; equilibration time = 45 seconds; λmax= 400 nm.

DCM showing maximum and steady absorbance is the ultimate choice.

Tabulation of physical parameters (acidity with respect to the aqueous phase, reagent concentration, and equilibration time) in Table 4 reflects the optimum conditions set for the formation of the complex and in the same form trace spectrophotometric determination of Nb (V).

Table 4. Effect of acidity, reagent concentration, and equilibration time on the absorbance of Nb(V)-HMC complex.

$HClO_4$[a](M)	0.4	0.8	1.2	1.6	2.0	2.16	2.24-3.28	3.36	3.52	3.76
Absorbance	0.282	0.321	0.365	0.402	0.479	0.490	0.510	0.490	0.454	0.400
HMC (ml)[b]	0.5	1	1.5	1.6	1.7-2.7	2.8	3.0	3.5		
Absorbance	0.117	0.359	0.510	0.524	0.530	0.513	0.501	0.416		
Equilibration time(seconds)[c]	0	2	5	10	15-300					
Absorbance	0.050	0.195	0.253	0.485	0.530					

Conditions: [a]Nb(V) = 10 µg; Acidity of the aqueous phase = variable; HMC [0.2% (w/v) in ethanol] = 1.5ml; aqueous volume = solvent volume = 10 ml; solvent = DCM; equilibration time = 45 seconds; λ_{max} = 400 nm. [b]Acidity of aqueous phase = 2.4 M; other conditions are the same as in (a) excepting variation in HMC concentration; [c]HMC [0.2% (w/v) in ethanol] = 2 ml; other conditions are the same as in (b) excepting variation in equilibration time

3.1. Selectivity of the method.

To assess the method's selectivity, the tolerance limits of varied foreign ions on complex formation are examined under the ideal conditions of the proposed approach. The anions or complexing agents are investigated as absorbance changes by mixing their readily available mg per 10 ml of sodium or potassium salts with 10 µg Nb (V) per 10 ml aqueous phase.

As evident from Table 5, of 22 anions, only oxalate, phosphate, and fluoride interfered seriously with the determination of Nb(V) as an HMC complex. Comparative investigations were performed for 34 different cations; as shown in Table 6, 33 cations did not obstruct the absorbance of Nb(V)-HMC complex when added alone or in the presence of masking or complexing agents. However, Sn(II) interfered seriously, raising absorbance to a much higher value by its presence. The utmost concentrations of a foreign ion that will cause a minor error were taken as the permissible level of the foreign ion.

Table 5. Effect of foreign ions – Anion/complexing agents.

S.No.	Anion/complexing agent	Tolerance limit (mg/10ml)	Absorbance
1	None	-	0.530
2	Sodium Bromide, Sodium Chloride, Potassium Iodide, Sodium Acetate, Sodium Nitrite, Sodium Carbonate, Sodium Sulphite, Potassium Thiocyanate, Thiourea, Ascorbic acid, Sulfosalicylic acid, Sodium Sulphite	100	0.530
3	'Disodium' EDTA, Hydrazine Sulphate, Sodium Dithionite	50	0.530
4	Sodium Potassium Tartrate, Sodium Nitrate	10	0.530
5	Hydrogen peroxide(30 %), Glycerol	1*	0.530
6	Sodium Oxalate**, Sodium Phosphate**, Potassium Fluoride**	0.1	0.214, 0.192, 0.112

*Amount added in ml; **Seriously interfered.

Table 6. Effect of foreign ions – Cations.

S.No.	Cations*	Tolerance limit (mg/10 ml)	Absorbance
1	None	-	0.530
2	Pb(II), Ba(II), Co(II) Mg(II), Cd(II), Zn(II), Ni(II),Ca(II), Ag(I)	10	0.530
3	Ce(IV), Se(IV), Cu(II), Hg(II), Mn(II)	5	0.530
4	Al(III)	2	0.530
5	Cr(VI),Zr(IV), Pt(IV), Ti(IV), La(III), Ir(III), Ru(III), Fe(III), Au(III), Bi(III), As(III), Pd(II), Sr(II), Fe(II)	1	0.530
6	W(VI)	0.5	0.530
7	Cr(III)	0.2	0.530
8	Mo(VI)[a], V(V)[b]	0.1	0.530
9	Sn(II)[c]	0.1	>2

*Initial oxidation state is shown in parentheses, [a]In presence of 100 mg Potassium thiocyanate; [b]In presence of 100 mg Ascorbic acid; [c]Interfered seriously.

3.2. Spectral and statistical characteristics.

Under the optimal conditions, the absorption spectrum of Nb(V) - HMC complex against reagent blank in DCM demonstrated the absorption maximum at 388-407 nm, where the spectrum of the reagent blank against pure DCM also exhibited a little absorbance, as is indicated in Figure 2.

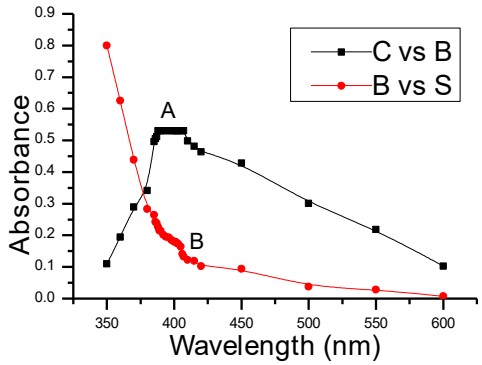

Figure 2. Absorption spectra of Nb (V) - HMC complex. **A** – Complex against reagent blank. **B** – Reagent blank against pure DCM. 1 µg Nb(V) ml^{-1}, other conditions cited in the procedure.

The Nb (V) - HMC complex obeys linearity over the concentration range 0.0-2.2 μg Nb(V) ml^{-1}(Figure 3) with the precise determination range as 0.395-1.78 ppm of Nb (V) as analyzed from Ringbom plot [31] (Figure 4). Via statistical approaches, various optical and statistical factors were analyzed and compiled in Table 7.

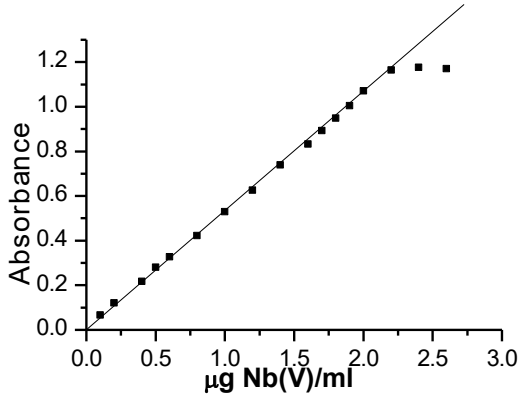

Figure 3. Beer's law range of Nb (V) - HMC complex in DCM at 400 nm.

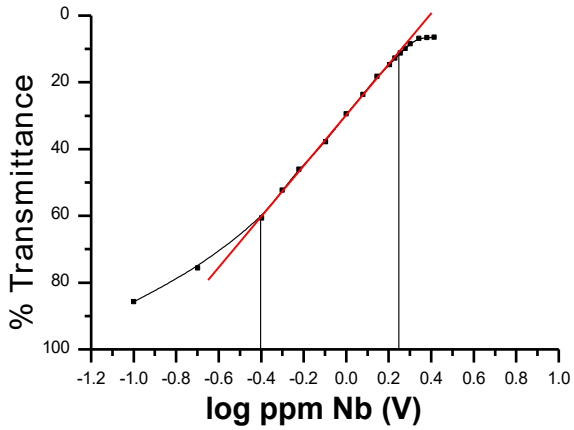

Figure 4. Ringbom plot for Nb (V) – HMCcomplex in DCM at 400 nm.

3.3. Stoichiometry of Nb (V) - HMC complex.

1:3 (M:L) stoichiometry of the studied complex is established by Job's continuous variations method as altered by Vosburgh and Cooper for a two-phase system, mole ratio, and equilibrium shift methods [32-35] (Figures 5-7).

Table 7. Spectral and Statistical data of Nb (V) - HMC complex.

Parameter	Value	Parameter	Value
Acidity of aqueous phase (M)	2.24-3.28	Sandell's sensitivity (μg cm^{-2})	0.0019
Reagent solvent	Ethanol	Correlation coefficient (r)	0.9994
Reagent concentration (0.2% w/v, ml)	1.7-2.7	Regression equation	Y = 0.514 X + 0.016
λ_{max} (nm)	388-407	Slope (b)	0.514
Extraction solvent	Dichloromethane	Intercept (a)	0.016
Equilibration time (Seconds)	15-300	Stoichiometry (M:L)	1:3
Beer's law limit [µg Nb(V) ml^{-1}]	0-2.2	Standard deviation	0.0012
Molar absorptivity (l mol^{-1} cm^{-1})	4.926×10^4	Relative standard deviation	0.2262
Limit of detection (μg ml^{-1})	0.0698	Stability of the complex	More than 4 days

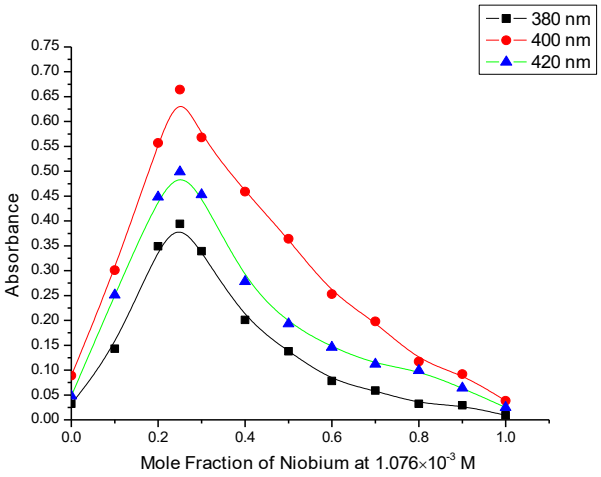

Figure 5. Job's continuous variations method.

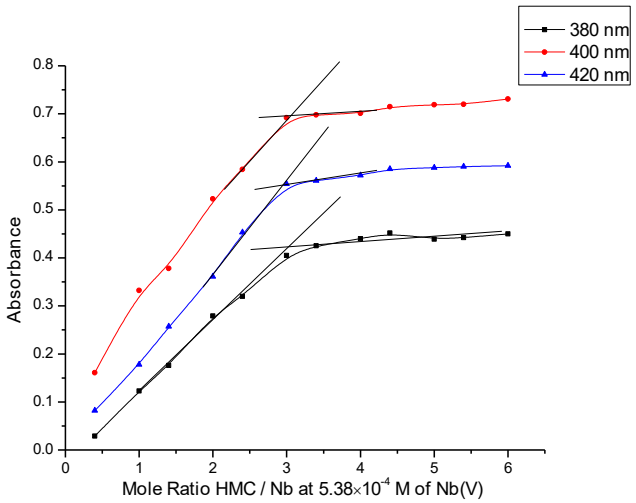

Figure 6. Mole - ratio method.

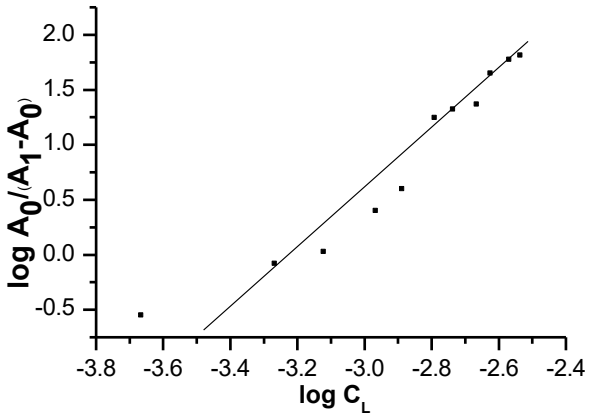

Figure 7. Equilibrium shift method; Concentration of the metal ion fixed = 5.38×10^{-4} M; Maximum absorbance, A_0 = 0.731; Study wavelength = 400 nm; Slope = 2.8.

The above three methods collectively indicate the following (Figure 8) proposed and optimized structure of the studied Nb(V)-HMCcomplex.

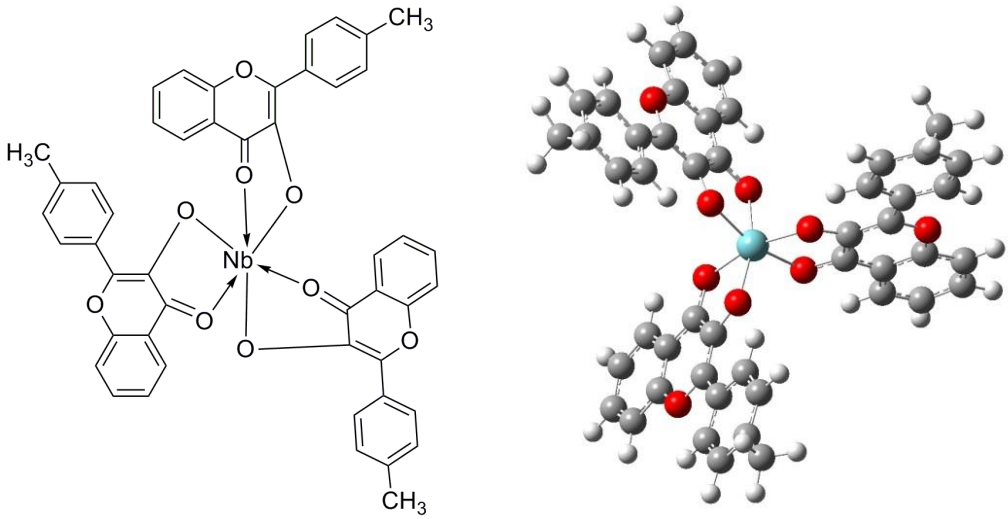

Figure 8. Proposed and optimized structure of Nb(V)-HMC complex.

3.4. FMO Analysis.

Physicists and chemists can be benefited from FMO (Frontier Molecular Orbitals) studies, the studies of molecular orbitals and their properties. To explain the optical and electronic properties of various molecules in chemistry, FMO analysis is commonly used. The HOMO and LUMO energies are extremely valuable in determining the chemical reactivity of the molecules. This is also utilized in frontier electron density to forecast the most reactive sites in multi-electron systems and explain various reactions and interactions in conjugated systems [36, 37]. Figure 9a and 9b illustrate the HOMO and LUMO, both for ligand, HMC, and the complex, Nb(V) - HMC.

Figure 9a. HOMO and LUMO of ligand, HMC.

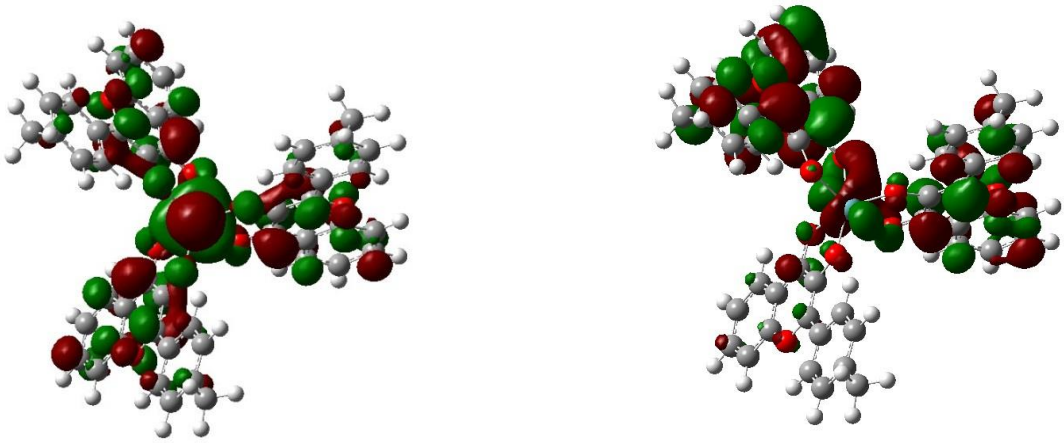

Figure 9b HOMO and LUMO of Complex, Nb(V)-HMC.

The LUMO receives electrons, and its energy correlates to the electron affinity (EA), whereas the HOMO represents electron donors with its energy corresponding to the ionization potential (IP) during molecular interactions. The HOMO-LUMO energy gap ΔE_{gap} is significant in identifying molecular electrical transport features expressing the final charge transfer interaction within the molecule. Because it is energetically unfavorable to add an electron to the low-lying LUMO in order to remove electrons from the high-lying HOMO, a molecule with a high frontier orbital gap (HOMO-LUMO energy gap) has low chemical reactivity and high kinetic stability [38-40]. Compounds with a large HOMO-LUMO energy gap, thus, are more stable and chemically tougher than those with a small HOMO-LUMO energy gap. The HOMO-LUMO energy gap increases from HMC to Nb(V)-HMC. The minimum energy gap is evaluated for ligand HMC. However, this gap increases in Nb(V)-HMC complex after three conjugated HMC rings approach pentavalent niobium for complexation. The presented study in the same context denotes a hard, more stable, and less reactive nature of Nb(V)-HMC complex with soft ligand HMC. The computed HOMO and LUMO energies are listed in Table 8.

Table 8. FMO Energies.

	HOMO (eV)	LUMO (eV)	ΔE_{gap} (eV)	Dipole moment (Debye)	Predicted energy change (Hartree)
HMC	-8.20514	-1.55714	6.64800	0.294095	-2.59×10^{-8}
Nb(V)-HMC	-9.89367	-0.62916	9.26451	6.058755	-7.93×10^{-4}

Global Reactivity descriptors [41-44] (Table 9) such as chemical potential (P_i), absolute electronegativities (χ), absolute hardness (η), global electrophilicity (ω), absolute softness (σ) and the fraction of electrons transferred (ΔN) were estimated both for HMC and its Nb (V) complex using following equations:

$$\omega = P_i^2 / 2\eta$$
$$P_i = -\chi$$
$$\eta = (E_{LUMO} - E_{HOMO})/2$$
$$\chi = -(E_{LUMO} + E_{HOMO})/2$$
$$\sigma = 1/\eta$$
$$\Delta N = -P_i/\eta$$

The global electrophilicity index (ω), introduced by Parr *et al.* [45,46], based on thermodynamic properties, is a measure of the favorable change in energy when a chemical system attains saturation by the addition of electrons. It can be defined as the decrease in energy due to the flow of electrons from the donor (HOMO) to the acceptor (LUMO) in molecules. It also plays an important role in determining the chemical reactivity of a system. It is the measure of the propensity of a species for its electron acceptance. High nucleophilicity and electrophilicity of compounds correspond to opposite ends of the scale of global reactivity indices, according to Domingo *et al.* [47], where the lower ω value denotes a good, more reactive nucleophile, and the higher is indicative of the good electrophile. Thus lower value for ligand HMC indicates the nucleophilic behavior favoring its complexation with positively charged niobium (V), resulting in the formation of the studied complex.

Table 9. Global Reactivity descriptors.

S. No.	Parameter	HMC	Nb(V) - HMC complex
1	χ(eV)	4.88114	5.26141
2	η(eV)	3.32399	4.63270
3	σ(eV^{-1})	0.30084	0.21586
4	P_i(eV)	-4.88114	-5.26141
5	ω(eV)	2.98772	3.58387
6	ΔN	1.46845	1.13571

Similarly, a larger negative value of work function (Pi) for Nb (V)-HMC complex indicates its greater stability and unwillingness to decompose its constituent metal ion and ligand.

Absolute hardness (η) and absolute softness (σ), denoted by high and low ΔE_{gap}, respectively, show HMC as a soft molecule and Nb(V)-HMC complex as a hard one, implying more ligand reactivity and hence the development of a stable and soft complex with low reactivity.

The molecular ability to attract electrons is studied in absolute electronegativity (χ). Electronegativity difference determines the charge transfer which occurs during bond formation. Also, the flow of electrons is generally from the atom with low electronegativity.

Low electronegativity (χ) value for HMC suggests electrons revocation to pentavalent niobium cation, indicating greater stability of the formed complex.

For HMC, ΔN or the fraction of electrons transferred is high, implying enough possibility of electron transfer from ligand to metal in the complex under study.

3.5. ESP analysis.

The ESP has a unique role in predicting and analyzing molecular recognition and is often helpful in demonstrating non-covalent molecular interactions [48,49]. By employing the ESP surface, in the color code range- 5.02×10^{-2} to $+ 5.02 \times 10^{-2}$eV, we can determine the spatial regions in molecular structure at which the electrostatic potential is negative or positive. This helps visualize charged regions of a molecule and is qualitatively useful in analyzing electrostatic interactions between the ligand and the central metal cation. Three-dimensional plots of the molecular electrostatic potentials of the studied ligand and the complex thus are illustrated in Figure 10, describing the compound's size, configuration, and charge density. The figure depicts the global maximum point associated with the HMC ligand having areas of positive potential (shown in blue color range) in front of the H-atoms arising from the lower electronegativity of these atoms, which is comparable to C-atoms. This is further noted that the most negative ESP region (in dark red), with a global minimum, is located around the hydroxyl and ketonic group of the benzopyran ring of the HMC ligand. This large negative value is due to the lone pair of electrons on the oxygen of the hydroxyl group in resonance with the adjacent ketonic group, thus delocalizing charge, making it nucleophilic, concluding that this region can be easily attracted by the region of positive potential or the pentavalent niobium cation.

In the ESP diagram of Nb(V)-HMC complex, the entire negative potential is observed over hydroxyl and ketonic groups of the benzopyran ring, thus acting as the donor ring, donating its electrons to positively charged niobium (V).

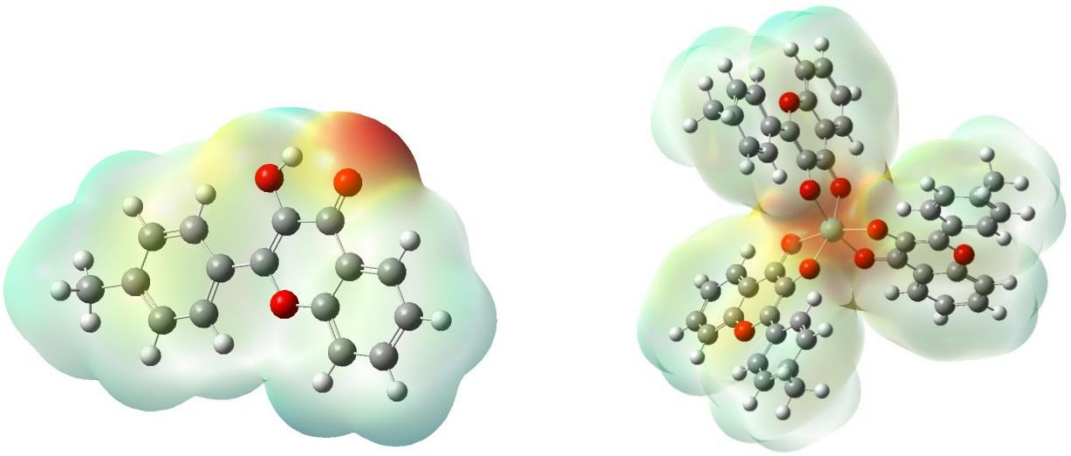

Figure 10. ESP mapped over the electron density isosurface for HMC and Nb(V) – HMC.

4. Conclusions

For the spectrophotometric determination of niobium (V) in traces, 3-hydroxy-2-(4-methylphenyl)-4H-chromen-4-one has been employed as an affluent analytical reagent. The metal in the presence of several cations and anions/complexing agents has been observed to give a yellow stable (stability more than 4 days) 1:3 complex with HMC, which is extractable into dichloromethane at 2.24-3.28 M concentration of HClO4 and 1.7-2.7 ml of 0.2% HMC solution in alcohol and showing an absorption maximum at 388-407 nm. The method has been

adopted for its simplicity, selectivity, rapidity, sensitivity with good precision and accuracy as indicated in comparison with existing methods of niobium determination (Table 10) and has been applied for the determination of niobium in numerous samples. Electronic properties of the formed complex are also studied with reference to the ligand as the FMO analysis indicates that the ligand has less HOMO-LUMO energy gap compared to its niobium (V) complex, making the complex kinetically stable, justifying thus the results obtained by spectrophotometric analysis. Further an extreme increase in the dipole moment values from ligand [HMC = 0.294095 Debye] to the complex [Nb(V) - HMC = 6.058755 Debye] proves higher stability of the complex. Lastly, ESP diagrams have helped greatly in elucidating the ligand and validating the donor sites coinciding with the spectrophotometric findings.

Table. 10 Comparison of the proposed method with the reported methods.

S.No.	Aqueous conditions	λ_{max} (nm), Solvent	Molar absorptivity (l mol^{-1} cm^{-1})	Interference	Ref.
1	Niobium (V), 2,6-dithiolphenol (DTP) and aminophenols (AP), pH-3.8-5.0	440, Chloroform	2.9×10^4	- (6 anions and 18 cations studied)	13
2	Niobium (V) with 2,4-dihydroxythiophenol (DHTP) and hydrophobic amines (HAs), Standing time;10 min, pH 4.3-5.0	430, Chloroform	$3.5\text{-}3.9 \times 10^5$	- (6 anions and 18 cations studied)	14
3	Nb(V)- 3-hydroxy-2-methyl-1 phenyl-4-pyridone, pH 3, xylenol orange	565, Chloroform Solution of Tetraphenylphosphonium Chloride	3.72×10^4	Selectivity not checked	15
4	Niobium (V)- 3-Hydroxy-2-(4'-methoxyphenyl)-4-oxo-4*H*-l-benzopyran (HMPB), $HClO_4$	405, Dichloromethane	3.764×10^4	Sn(II)	16
5	Niobium (V), Oxine and Naphthalene, Basic Medium	380 -	1.40×10^4	- (9 anions and 22 cations studied)	17
6	Nb (V), 3-Hydroxy-2-(4-methylphenyl)-4*H*-chromen-4-one, pH 1.01-2.25	400, Dichloromethane	4.926×10^4	Oxalate, Phosphate, Fluoride, Sn(II) of 22 anions and 34 cations studied	Proposed Method

Funding

This research received no external funding.

Acknowledgments

Thanks sincerely to the officials, Maharishi Markandeshwar (Deemed to be University), Mullana, for providing the necessary resources to carry out the framed work.

Conflicts of Interest

No conflict of interest is declared by the authors.

References

1. Heisterkamp, F.; Carneiro, T. Niobium: Future possibilities- technology and market place. *Niobium sci technol proc int sym niobium, Orlando,* Florida, USA **2002.**
2. Gupta, C. K.; Suri, A. K. Extractive Metallurgy of Niobium. *CRC Press E,* New York, USA, **1994**, https://doi.org/10.1201/9780203756270.
3. Enginsoy, H.M., Bayraktar, E., Gatamorta, F., Katundi, D., Miskioglu, I. Recycled Niobium-Aluminium (Nb2Al) Intermetallics Based Composite Design: An Experimental and Numerical Approach for Toughening Mechanism. In: Chalivendra, V., Beese, A.M., Berke, R.B, Eds.; Mechanics of Composite, Hybrid and Multifunctional Materials, Fracture, Fatigue, Failure and Damage Evolution. Conference Proceedings of the Society for Experimental Mechanics Series. *CPSEMS Springer* **2022,** *3*, 71-79, https://doi.org/10.1007/978-3-030-86741-6_12.
4. Mallela, V.S.; Ilankumaran, V.; Rao, N. S. Trends in Cardiac Pacemaker Batteries. *Ind Pacing Electrophysiol J* **2004**, *4*, 201-212.
5. Godley, R.; Starosvetsky, D.; Gotman, I. Corrosion behavior of a low modulus β-Ti-45%Nb alloy for use in medical implants. *J Mater Sci : Mater in Med.* **2006**, *17*, 63-67, https://doi.org/10.1007/s10856-006-6330-6.
6. Dhonchak, C.; Agnihotri, N.; Kumar, A. Zirconium (IV)-3-hydroxy-2-tolyl-4*H*-chromen-4-one complex—the analytical and DFT studies. *J Mol Model* **2021**, *27*, 336, https://doi.org/10.1007/s00894-021-04949-0.
7. Dhonchak, C.; Kaur, N.; Agnihotri, R.; Berar, U.; Agnihotri, N. Trace Determination of Zirconium (IV) as its 3-Hydroxy-2-[2′-(5′-Methylthienyl)]-4*H*-Chromen-4-One Complex and Structural Elucidation by Quantization Technique. *Mobile Radio Communications and 5G Networks LNNS* **2021**, *140*, 333-344, https://doi.org/10.1007/978-981-15-7130-5_25.
8. Shiwani, S.; Agnithotri, N.; Rathi, P.; Agnihotri, R.; Kumar, V. Molecular Dynamics, Biological Study and Extractive Spectrophotometric Determination of Vanadium (V)-2-methyl-8-quinolinol Complex. *Iran J Chem Chem Engg* **2021**, *40*, 207-214, https://doi.org/10.30492/IJCCE.2020.93050.3273.
9. Kaur, N.; Agnihotri, N.; Agnihotri. R. 3-Hydroxy-2-[2'-(5'-methylthienyl)]-4-oxo-4*H*-1-benzopyran for the spectrophotometric determination of Tungsten(VI) and Palladium(II). *Vietnam J Chem* **2019**, *57*, 686-695, https://doi.org/10.1002/vjch.201900069.
10. Agnihotri, R.; Singh, A.; Agnihotri, N. Extraction and Spectrophotometric Determination of Molybdenum (VI) using 3-hydroxy-2-[3-(4-methoxyphenyl)-1-phenyl-4-pyrazolyl]-4-oxo-4H-1-benzopyran as a Chelating Agent. *J Anal Chem* **2019,** *74*, 81-86, https://doi.org/10.1134/S1061934819010027.
11. Rathi, P.; Garg, A,; Khanna, R. 4, 4'-Diantipyrylmethane (DAM): A tool for spectrophotometric microdetermination of cerium (IV). *Res J Chem Environ* **2021,** *25*, 49-55, https://doi.org/10.25303/257rjce4921.
12. Shokrollahi, A.; Ghaedi, M.; Niband, M.S.; Rajabi, H.R. Selective and sensitive spectrophotometric method for determination of sub-micro-molar amounts of aluminium ion. *J Hazard. Mat* **2008**, *151*, 642-648, https://doi.org/10.1016/j.jhazmat.2007.06.037.
13. Kuliyev, K. A.; Nailya, A. V. Spectroscopic Investigation of the Complex Formation of Niobium Using 2,6-Dithiolphenol and Aminophenols. *American J Anal Chem* **2015,** *6*, 746-756, https://doi.org/10.4236/ajac.2015.69071.
14. Zalov, A. Z. Complex Formation and Liquid-Liquid Extraction in the Niobium(V) – 2,4-Dihydroxythiophenol– Hydrophobic Amines System. *Pakistan J Anal Environ Chem* **2015**, *16*, 19-27.
15. Gojmerac, A.; Galic, N.; Tomisic. V. Formation and Extraction of Niobium(V) Complex with Xylenol Orange in the Presence of a 4-Pyridone Derivative. *J Solut Chem* **2009**, *38*, 149-158, https://doi.org/10.1007/s10953-008-9363-2.
16. Agnihotri, N.; Agnihotri. R. Extractive Spectrophotometric Determination of Niobium (V) Using 3-Hydroxy-2-(4'-Methoxyphenyl)-4-Oxo-4H-l-Benzopyran as a Complexing Agent. *The Open Anal Chem* **2012**, *6*, 39-44, https://doi.org/10.2174/1874065001206010039.
17. Hamed, M.M.; Aglan, R.F.; El-Reefy, S.A. Normal and second derivative spectrophotometric determination of niobium using solid phase extraction technique. *J Anal Chem* **2015,** *70*, 1103-1110, https://doi.org/10.1134/S1061934815090075.
18. Uddin, M.A.; Sutonu, B.H.; Rub, M.A.; Mahbub, S.; Alotaibi, M. M.; Asiri, A. M.; Rana, S.; Hoque, Md. A.; Kabir, M. UV-Visible spectroscopic and DFT studies of the binding of ciprofloxacin hydrochloride antibiotic drug with metal ions at numerous temperatures. *Korean J Chem Eng* **2022**, *39*, 664-673, https://doi.org/10.1007/s11814-021-0924-z.

19. Saranya, B.; Gowri, M. Synthesis, Characterization, DFT study and Molecular Docking of (Z)-4-((2-hydroxy-3-methoxy benzylidene)amino)-1,5-dimethyl-2-phenyl-1,2-dihydro-3H-pyrazol-3-one and its Metal Complexes. *J Mol Struc* **2022,** *1250*, 131674, https://doi.org/10.1016/j.molstruc.2021.131674.
20. Gammal, O.A.E.; Bindary, A. A. E.; Sh. Mohamed, F.; Rezk, G. N.; El-Bindary, M. A. Synthesis, characterization, design, molecular docking, anti COVID-19 activity, DFT calculations of novel Schiff base with some transition metal complexes. *J Mol Liq* **2022,** *346*, 117850, https://doi.org/10.1016/j.molliq.2021.117850.
21. Kherrouba, A.; Bensegueni, R.; Guergouri, M.; Boulkedid, A-L.; Boutebdja, M.; Bencharif, M. Synthesis, crystal structures, optical properties, DFT and TD-DFT studies of Ni (II) complexes with imine-based ligands, *J Mol Struc* **2022**, *1247*,131351, https://doi.org/10.1016/j.molstruc.2021.131351.
22. Abu-Dief, A.M.; El-Khatib, R. M.; Aljohani, F. S.; Al-Abdulkarim, H. A.; Alzahrani, S.; El-Sarrag, G.; Ismael, M. Synthesis, structural elucidation, DFT calculation, biological studies and DNA interaction of some aryl hydrazone Cr^{3+}, Fe^{3+}, and Cu^{2+} chelates, *Comput Biol Chem* **2022**, *97*, 107643, https://doi.org/10.1016/j.compbiolchem.2022.107643.
23. Algar, J.; Flynn, J.P. A new method for the synthesis of flavonols. *Proc Royal Irish Acad* **1934**, *42B*, 1-7.
24. Oyamada, T. A new general method for the synthesis of flavonol derivatives. *J Chem Soc Jpn* **1934**, *55*, 1256-1261.
25. Padgett, W. C.; Lynch, K.; Sheriff, W. E.; Dean, R.; Zingales, S. 3-Hydroxy-2-(4-methylphenyl)-4*H*-chromen-4-one. *IUCr* **2018**, *3*, 181138, https://doi.org/10.1107/S2414314618011380.
26. Miar, M.; Shiroudi, A.; Pourshamsian, K.; Oliaey, A.R.; Hatamjafari, F. Theoretical investigations on the HOMO–LUMO gap and global reactivity descriptor studies, natural bond orbital, and nucleus-independent chemical shifts analyses of 3-phenylbenzo[d]thiazole-2(3H)-imine and its para-substituted derivatives: Solvent and substituent effects. *J Chem Res* **2021,** *45*, 147-158, https://doi.org/10.1177/1747519820932091.
27. Guzel, E.; Demircioğlu, Z.; Ağar, E.; Çicek, C.; Yavuz, M. Experimental (XRD, FTIR, UV–Vis, NMR) and theoretical investigations (chemical activity descriptors, NBO, DNA/ECT) of (E)-2-((2-hydroxy-5-methoxybenzylidene)amino)-4-nitrophenol, *Mol Crys Liq Crys* **2021,** *724*, 58-76, https://doi.org/10.1080/15421406.2021.1905143.
28. Frisch, M. J. et al., GAUSSIAN 09, Revision A.02, Gaussian, Inc., Wallingford, CT **2009**.
29. Dennington, R.; Keith, T.; Millam, J. GaussView, Version 5, Semichem Inc., Shawnee Mission, KS **2009**.
30. Shiroudi, A.; Safaei, Z.; Kazeminejad, Z.; Repo, E.; Pourshamsian, K. DFT study on tautomerism and natural bond orbital analysis of 4-substituted 1,2,4-triazole and its derivatives: solvation and substituent effects. *J Mol Model* **2020**, *26*, 57, https://doi.org/10.1007/s00894-020-4316-9.
31. Ringbom, A. On the accuracy of colorimetric analytical methods. *J Anal Chem* **1938,** *115*, 332-343.
32. Job, P. Formation and stability of inorganic complexes in solution. *Ann Chim* **1928,** *9*, 113-134.
33. Vosburgh, W. C.; Cooper, G. C. The identification of complex ion in solution by spectrophotometric measurements. *J Am Chem Soc* **1941,** *63*, 437-442, https://doi.org/10.1021/ja01847a025.
34. Yoe, J. H.; Jones, A. L. Colorimetric determination of iron with disodium-1,2-dihydroxybenzene-3,5-disulfonate. *Ind Eng Chem (Anal Ed)* **1944,** *16*, 111-115, https://doi.org/10.1021/I560126A015.
35. Tarasiewicz, H. P.; Grudiniewska A.; Tarasiewicz, M. An examination of chlorpromazine hydrochloride as indicator and spectrophotometric reagent for the determination of molybdenum(V). *Anal Chim Acta* **1977**, *94*, 435-442, https://doi.org/10.1016/S0003-2670(01)84546-3.
36. Seeman, J. I.; Fukui, K. Frontier Molecular Orbital Theory, and the Woodward-Hoffmann Rules. Part II. A Sleeping Beauty in Chemistry. *Chem. Rec.* **2022**, *22* , e202100245, https://doi.org/10.1002/tcr.202100300.
37. Singh, J.S.; Khan, M.S.; Uddin, S. A DFT study of vibrational spectra of 5-chlorouracil with molecular structure, HOMO–LUMO, MEPs/ESPs and thermodynamic properties. *Polym Bull* **2022**, *79*, https://doi.org/10.1007/s00289-022-04181-7.
38. Nakakuki, Y.; Hirose, T.; Matsuda, K. Logical Design of Small HOMO–LUMO Gap: Tetrabenzo[f,jk,mn,r][7] helicene as a Small-Molecule Near-Infrared Emitter. *Org Lett* **2022**, *24*, 648-652, https://doi.org/10.1021/acs.orglett.1c04095.
39. Kanagathara, N.; Usha, R.; Natarajan, V.; Marchewka, M.K. Molecular geometry, vibrational, NBO, HOMO–LUMO, first order hyper polarizability and electrostatic potential studies on anilinium hydrogen oxalate hemihydrate – an organic crystalline salt. *Inorg Nano-Met Chem* **2021,** *52*, 226-233, https://doi.org/10.1080/24701556.2021.1891103.

40. Verma, V. K.; Guin, M.; Solanki, B.; Singh, R. C. Molecular structure, HOMO and LUMO studies of Di (Hydroxybenzyl) diselenide by quantum chemical investigations. *Mat Proc* **2022,** *49*, 3200-3204, https://doi.org/10.1016/j.matpr.2020.11.887.
41. Ekennia, A.C.; Onwudiwe, D.C.; Osowole, A.A.; Okpareke, O.C.; Olubiyi, O.O.; Lane, J.R. Coordination compounds of heterocyclic bases: synthesis, characterization, computational and biological studies. *Res Chem Intermed* **2019**, *45*, 1169–1205, https://doi.org/10.1007/s11164-018-3664-x.
42. Vektariene, A.; Vektaris, G.; Svoboda, J. A theoretical approach to the nucleophilic behavior of benzofused thieno[3,2-b]furans using DFT and HF based reactivity descriptors. *Arkivoc* **2009**, *7*, 311-329.
43. Zayed, E. M.; El-Samahy, F. A.; Mohamed, G.G. Structural, spectroscopic, molecular docking, thermal and DFT studies on metal complexes of bidentate orthoquinone ligand. *Appl Organomet Chem* **2019,** *33*, e5065, https://doi.org/10.1002/aoc.5065.
44. Mahmoud, W. H.; Sayed, F. N.; Mohamed, G. G. Synthesis, characterization and in vitro antimicrobial and anti-breast cancer activity studies of metal complexes of novel pentadentate azo dye ligand. *Appl Organomet Chem* **2016**, *30*, 959-973. https://doi.org/10.1002/aoc.3529.
45. Jalezadeh, A.; Mirjafary, Z.; Rouhani, M.; Saeidian, H. Investigation of structural, electronic, and antioxidant properties of calycopetrin and xanthomicrol as two polymethoxylated flavones using DFT calculations. *Struct Chem* **2022**, *33*, 1241-1250, https://doi.org/10.1007/s11224-022-01929-9.
46. Mohmad, M.; Agnihotri, N.; Kumar, V.; Kumar, R.; Kaviani, S. Iridium(III)-3-hydroxy-2-(3′-methyl-2′-thienyl)-4-oxo-4*H*-1-benzopyran complex: The analytical, in-vitro antibacterial and DFT studies. *Inorg Chem Comm* **2022,** *139*, 109333, https://doi.org/10.1016/j.inoche.2022.109333.
47. Domingo, L.R.; Aurell, M.J.; Perez, P.; Contreras, R. Quantitative characterization of the global electrophilicity power of common diene/dienophile pairs in Diels–Alder reactions. *Tetrahedron* **2002**, *58*, 4417-4423, https://doi.org/10.1016/S0040-4020(02)00410-6.
48. Chiu, T. P.; Rao, S.; Mann, R.S.; Honig, B.; Rohs, R. Genome-wide prediction of minor-groove electrostatic potential enables biophysical modeling of protein–DNA binding. *Nucl Acids Res* **2017**, *45*, 12565-12576. https://doi.org/10.1093/nar/gkx915.
49. Zahid, S.; Rasoola, A.; Ayuba, A. R.; Ayub, K.; Iqbal, J.; Al-Buriahid, M. S.; Alwadaie, N.; Somaily, H. H. Silver cluster doped graphyne (GY) with outstanding non-linear optical properties. *RSC Adv* **2022,** *12*, 5466-5482, https://doi.org/10.1039/D1RA08117A.